AGU PUBLICATIONS

Geophysical Research Letters

RESEARCH LETTER
10.1002/2016GL069225

Special Section:
First results from NASA's Magnetospheric Multiscale (MMS) Mission

Decay of mesoscale flux transfer events during quasi-continuous spatially extended reconnection at the magnetopause

H. Hasegawa[1], N. Kitamura[1], Y. Saito[1], T. Nagai[2], I. Shinohara[1], S. Yokota[1], C. J. Pollock[3,4], B. L. Giles[3], J. C. Dorelli[3], D. J. Gershman[3,5], L. A. Avanov[3], S. Kreisler[3], W. R. Paterson[3], M. O. Chandler[6], V. Coffey[6], J. L. Burch[7], R. B. Torbert[8], T. E. Moore[3], C. T. Russell[9], R. J. Strangeway[9], G. Le[3], M. Oka[10], T. D. Phan[10], B. Lavraud[11,12], S. Zenitani[13], and M. Hesse[3]

[1]Institute of Space and Aeronautical Science, Japan Aerospace Exploration Agency, Sagamihara, Japan, [2]Tokyo Institute of Technology, Tokyo, Japan, [3]NASA Goddard Space Flight Center, Greenbelt, Maryland, USA, [4]Now at Denali Scientific, Healy, Alaska, USA, [5]Oak Ridge Associated Universities, Washington, District of Columbia, USA, [6]NASA Marshall Space Flight Center, Huntsville, Alabama, USA, [7]Southwest Research Institute, San Antonio, Texas, USA, [8]Space Science Center, University of New Hampshire, Durham, New Hampshire, USA, [9]Department of Earth, Planetary, and Space Sciences, University of California, Los Angeles, California, USA, [10]Space Sciences Laboratory, University of California, Berkeley, California, USA, [11]Institut de Recherche en Astrophysique et Planétologie, Université de Toulouse, Toulouse, France, [12]Centre National de la Recherche Scientifique, Toulouse, France, [13]National Astronomical Observatory of Japan, Mitaka, Japan

Key Points:
- Evidence of quasi-continuous and spatially extended magnetopause reconnection for southward IMF
- Broadening toward the magnetosphere of the reconnection jet with distance from the X line
- Mesoscale flux transfer events decay as the jet evolves with distance from the X line

Correspondence to:
H. Hasegawa,
hase@stp.isas.jaxa.jp

Citation:
Hasegawa, H., et al. (2016), Decay of mesoscale flux transfer events during quasi-continuous spatially extended reconnection at the magnetopause, *Geophys. Res. Lett.*, *43*, 4755–4762, doi:10.1002/2016GL069225.

Received 14 MAR 2016
Accepted 28 APR 2016
Accepted article online 4 MAY 2016
Published online 21 MAY 2016
Corrected 13 JUN 2016

This article was corrected on 13 JUN 2016. See the end of the full text for details.

Abstract We present observations on 2 October 2015 when the Geotail spacecraft, near the Earth's equatorial plane, and the Magnetospheric Multiscale (MMS) spacecraft, at midsouthern latitudes, simultaneously encountered southward jets from dayside magnetopause reconnection under southward interplanetary magnetic field conditions. The observations show that the equatorial reconnection site under modest solar wind Alfvén Mach number conditions remained active almost continuously for hours and, at the same time, extended over a wide range of local times (≥4 h). The reconnection jets expanded toward the magnetosphere with distance from the reconnection site. Geotail, closer to the reconnection site, occasionally encountered large-amplitude mesoscale flux transfer events (FTEs) with durations about or less than 1 min. However, MMS subsequently detected no or only smaller-amplitude corresponding FTE signatures. It is suggested that during quasi-continuous spatially extended reconnection, mesoscale FTEs decay as the jet spatially evolves over distances between the two spacecraft of ≥350 ion inertial lengths.

1. Introduction

Magnetic reconnection is a fundamental plasma process that changes the topology of magnetic field lines and converts magnetic energy into plasma kinetic and thermal energies. When this process occurs at the magnetopause, mass, momentum, and energy of the solar wind are efficiently transferred into the magnetosphere [e.g., *Dungey*, 1961]. Magnetopause reconnection can have an X line extended over a wide range of magnetic local time (MLT) [e.g., *Phan et al.*, 2006; *Dunlop et al.*, 2011] and can last for hours under high magnetic shear conditions [*Frey et al.*, 2003; *Phan et al.*, 2004; *Hasegawa et al.*, 2008]. However, it remains unclear whether magnetopause reconnection can be spatially extended and continuous at the same time.

Flux transfer events (FTEs), characterized by bipolar variations of the magnetic field component normal to the nominal magnetopause and enhancements of the field intensity [*Russell and Elphic*, 1978], are signatures of a time-dependent form of magnetopause reconnection [e.g., *Scholer*, 1995; *Paschmann et al.*, 2013]. FTEs have been observed even when magnetopause reconnection is continuous, which *Phan et al.* [2004] interpreted as being due to temporal variations of the rate of continuous reconnection. FTEs can be a channel for efficient entry of solar wind plasmas into the magnetosphere [e.g., *Sibeck and Siscoe*, 1984] and, if multiple X lines are involved, may be an agent to suppress tailward transport of the reconnected field lines [*Hasegawa et al.*, 2010]. It is thus important to understand the generation and evolution processes and the fate of FTEs. However, it has been difficult to address this issue because same FTEs are rarely observed by multiple probes situated at locations separated largely in the latitudinal or longitudinal direction (see *Wang et al.* [2007] for such a case of near-simultaneous FTE encounter by multiple spacecraft).

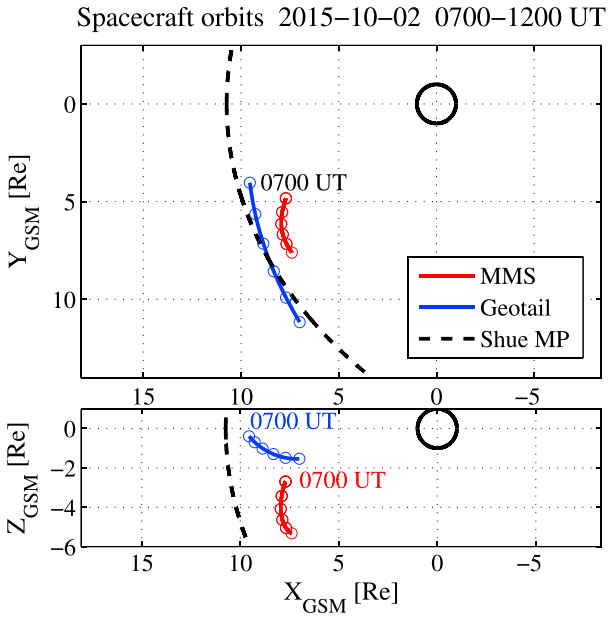

Figure 1. Orbits in GSM of the Geotail and MMS spacecraft during a 5 h interval 0700–1200 UT on 2 October 2015, along with the position of a model magnetopause [*Shue et al.*, 1998].

In this letter, we present simultaneous observations on 2 October 2015 by the Geotail and Magnetospheric Multiscale (MMS) [*Burch et al.*, 2016] spacecraft of the Earth's dayside magnetopause, which show that reconnection at the equatorial magnetopause can be quasi-continuous and spatially extended at the same time. A few FTEs were encountered by both sets of the spacecraft located at different latitudes, allowing us to investigate spatial development of FTEs. We use ion and magnetic field data from Geotail and MMS. The MMS data used in this paper are from the fast-survey mode and have 4.5 s resolution for the Fast Plasma Investigation (FPI) ion measurement [*Pollock et al.*, 2016], unless otherwise stated, and 16 Hz sampling for magnetic fields from the magnetometers (FGM) [*Russell et al.*, 2016]. Since the separation of the four MMS spacecraft was ~25 km, smaller than ion inertial length (~50 km) in the magnetosheath, we show MMS data from one spacecraft (MMS-1) only, but data from all four spacecraft are used. Ion density values from Geotail are doubled in the present study, taking into account saturation of the detector in intense ion flux regions and the fact that for the interval of interest, the magnetosheath density from MMS was about twice the uncorrected density from Geotail.

2. Observations of Quasi-Continuous and Extended Magnetopause Reconnection

The present observations were made on 2 October 2015, when Geotail was skimming the dayside equatorial magnetopause and MMS was at or near the postnoon magnetopause at midsouthern latitudes (Figure 1). Observations by the Wind spacecraft show that the interplanetary magnetic field (IMF) was persistently southward and duskward for a 5 h interval 0700–1200 UT, and the upstream solar wind parameters were quasi-steady, with an Alfvén Mach number of 4–6 (Figures 2a–2c). Magnetopause crossings, which can be identified by jumps in the ion density, temperature, and the L component of the magnetic field, often occurred nearly simultaneously for the two sets of spacecraft (Figure 2). The LMN coordinate system [*Russell and Elphic*, 1978] for each spacecraft was determined by minimum variance analysis of the magnetic field (MVAB) [*Sonnerup and Scheible*, 1998], applied to the entire 5 h interval of data. Although the normal N direction may differ at different MLTs, the main focus here is the L components of the magnetic field and velocity which are not sensitive to choices of the MVAB interval. The near-simultaneous crossings were generally due to modest time variations in the solar wind dynamic pressure (Figure 2c).

Both Geotail and MMS observed high-speed ion flows on the order of the magnetosheath Alfvén speed ~250 km/s in regions earthward of almost all the magnetopause crossings (only one exception is the crossing by Geotail at 0758 UT). These flows, often with speeds comparable to or exceeding the upstream solar wind speed (~380 km/s), were oriented approximately southward or in the $-L$ direction (Figures 2f and 2i). They are not magnetosheath flows deflected away from the subsolar region, because the magnetosheath flow speeds never reach these levels in those longitudinal and latitudinal locations of Geotail and MMS [*Lavraud et al.*, 2013, and references therein].

We identified both fluid and kinetic signatures of magnetopause reconnection. Figures 3a and 3c show Walén plots for typical magnetopause crossings by Geotail and MMS, respectively. The Walén relation [*Sonnerup et al.*, 1987] is satisfied sufficiently well with slopes close to −1, consistent with a rotational discontinuity magnetopause where the magnetic field component B_N normal to the boundary is locally positive.

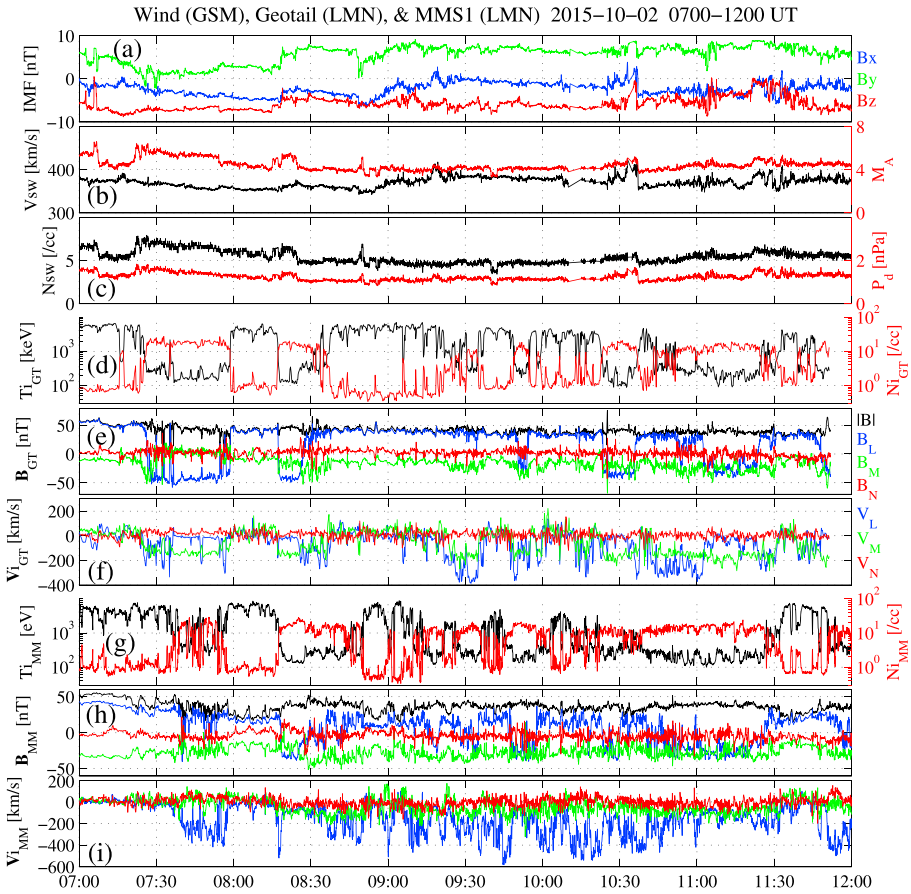

Figure 2. Solar wind and IMF conditions seen by the Wind spacecraft, time shifted by 75 min to take into account the propagation time from Wind to Geotail, and ion and magnetic field data taken by Geotail (12 s resolution for ions and 3 s average for fields) and MMS-1 (4.5 s average). (a) GSM components of the IMF, (b) solar wind speed and Alfvén Mach number, (c) solar wind density and dynamic pressure, (d–f) ion density and temperature, magnetic field and ion velocity from Geotail in *LMN*, and (g–i) those from MMS-1. GSM components of the *LMN* axes are: $\mathbf{L}_{GT}$ = [0.213, 0.029, 0.977], $\mathbf{M}_{GT}$ = [0.504, −0.859, −0.085], and $\mathbf{N}_{GT}$ = [0.837, 0.511, −0.197] for Geotail, and $\mathbf{L}_{MM}$ = [0.685, −0.007, 0.729], $\mathbf{M}_{MM}$ = [0.059, −0.996, −0.065], and $\mathbf{N}_{MM}$ = [0.726, 0.088, −0.682] for MMS-1.

This indicates that both spacecraft were on reconnected field lines southward of the reconnection site. Figures 3e and 3f show MMS-1 burst-mode measurements of ion velocity distributions on the magnetospheric and magnetosheath sides of the crossing analyzed in Figure 3c (three-dimensional distribution functions are not available from Geotail for the interval of interest). D-shaped distributions in the high-speed jet region and reflected components of magnetosheath protons, with cutoff at magnetic field-aligned velocities comparable to or exceeding the Alfvén speed, are both ion kinetic signatures of reconnection [*Fuselier*, 1995, and references therein] and indicate that MMS was on the reconnected field lines.

Figures 3b and 3d show scatterplots for Geotail and MMS, respectively, of the *L* component of ion velocities versus that of the magnetic fields, with ion densities represented by colors. It is evident that the V_L magnitude increases with increasing B_L, that is, as one crosses the magnetopause from the magnetosheath into the magnetosphere. The density in the magnetopause transition region ($B_L \sim 0$) is comparable to, or somewhat lower than, the magnetosheath value, consistent with a rotational discontinuity magnetopause. These features indicate that the Walén relation roughly holds for almost all the crossings. Some of the high-density data points are scattered along the V_L axis at similar B_L values. This is mostly due to time variations of the magnetosheath field or flow conditions, because the Walén relation is satisfied for shorter intervals. The nearly persistent Alfvénic southward flows in and earthward of the magnetopause demonstrate that the dominant reconnection line was northward of Geotail and MMS, and it was active almost continuously for the 5 h interval.

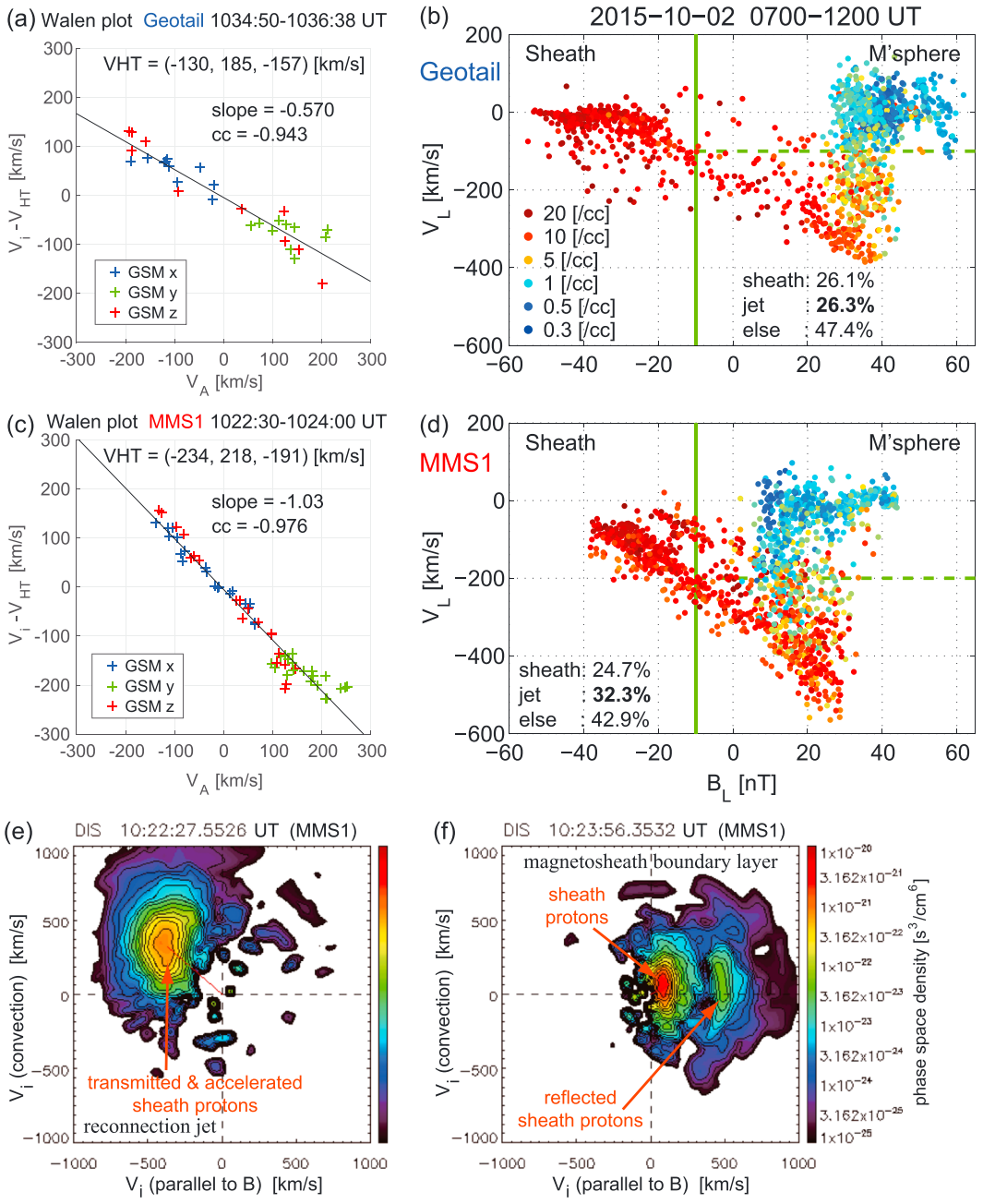

Figure 3. Walén relations for magnetopause crossings by (a) Geotail and (c) MMS-1, showing GSM components of ion velocity in the deHoffmann-Teller (HT) frame versus those of the local Alfvén velocity. The estimated HT velocity is also shown. Scatterplots of the L component of ion velocities versus that of the magnetic field, with densities represented by color, for (b) Geotail and (d) MMS. The probabilities of detecting either of the magnetosheath ($B_L < -10$ nT), reconnection jet ($B_L > -10$ nT, ion density $N_i > 1$ cm^{-3}, and $V_L < -100$ km/s for Geotail and $V_L < -200$ km/s for MMS), and magnetospheric or boundary layer regions (everything else) are shown in numbers. The time resolution of data used here is 12 s for both Geotail and MMS-1. 2-D cuts at the plane containing ion bulk velocity vector of ion velocity distributions seen by MMS-1 in the burst mode on the (e) magnetospheric and (f) magnetosheath sides of the crossing shown in Figure 3c. The Walén test intervals and times of the velocity distribution measurements are marked in Figure 4.

Note that on the magnetosheath side, V_L at MMS has a negative offset of about −100 km/s, as compared to V_L at Geotail. This is a real, rather than instrumental, effect due to the midlatitude locations of MMS where the magnetosheath flows diverted from the subsolar region with appreciable southward and tailward components are observed. We also see that the $|V_L|$ increase seen by Geotail is smaller than seen by MMS.

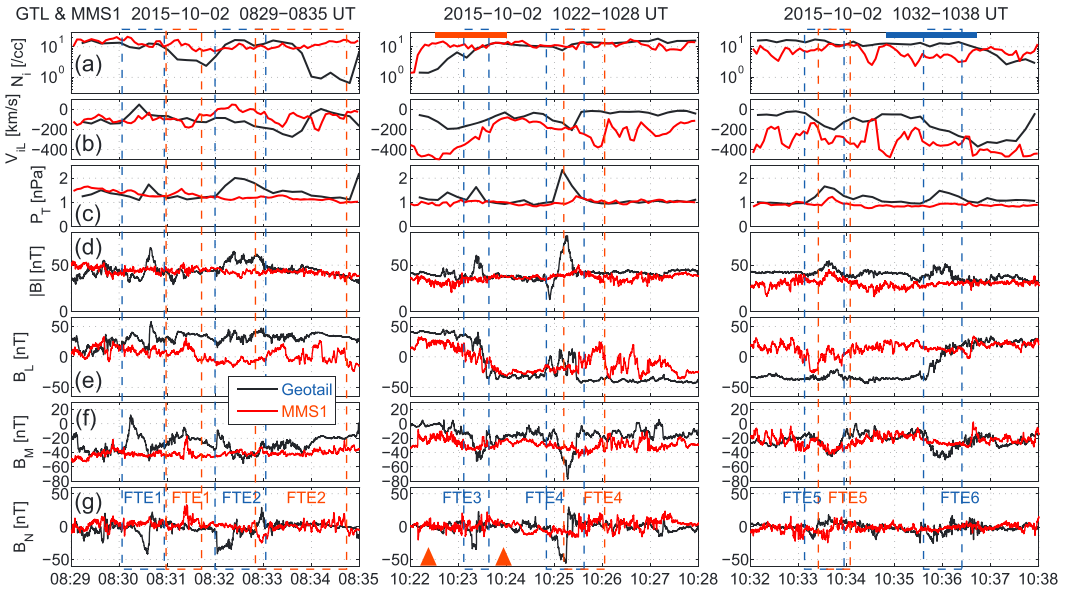

Figure 4. Geotail (black) and MMS-1 (red) observations when Geotail encountered mesoscale large-amplitude FTEs. (a) Ion density, (b) *L* component of the ion velocity, (c) total (ion plus magnetic) pressure, and (d–g) intensity and *LMN* components of the magnetic field. The blue and red bars in Figure 4a mark the intervals of the Walén test shown in Figures 3a and 3c, respectively. Two red triangles in Figure 4g indicate the times when the velocity distributions in Figures 3e and 3f were recorded.

This is partially because the Geotail ion instrument lacks fields of view in the spin-axis (approximately north-south) directions [*Mukai et al*., 1994], so that the V_z magnitude may be underestimated. The larger $|V_L|$ jump at MMS may also partially have resulted from acceleration during the jet evolution from the Geotail to MMS latitudes due to spatial gradients (pressure gradient and/or mirror force).

We note that Geotail moved from the subsolar part of the magnetopause to $y = +11\ R_E$ during the interval in question (Figure 1) and that Geotail observed reconnection jets near the subsolar point during an earlier interval (~0300 UT) when the IMF condition was similar (not shown). It indicates that the dominant X line northward of Geotail extended all the way from the subsolar region to $y = +11\ R_E$. In summary, the simultaneous Geotail and MMS observations demonstrate that magnetopause reconnection under southward IMF conditions remained active for hours and its reconnection line was extended over ≥4 h of MLT.

3. Broadening of the Reconnection Jets

We identified signatures consistent with broadening toward the magnetosphere of the reconnection jets with distance from the X line. Figures 3b and 3d show that there are a larger number of red (high-density) points in the magnetopause ($B_L \sim 0$) and on the magnetospheric side for MMS than Geotail. To be more precise, the data points are divided into three categories characterizing the magnetosheath, reconnection jet, and magnetospheric or boundary layer regions (see Figure 3 caption for details). The results indicate that the magnetosheath region was encountered by Geotail and MMS with a roughly equal detection probability and, importantly, that the jet region was seen more frequently by MMS (32.3%) than Geotail (26.3%). We thus conclude that the outflow jets were wider along the magnetopause normal at the location of MMS than Geotail and that the jet region expanded earthward during its evolution.

4. Decay of Mesoscale Flux Transfer Events

By surveying high time (16 Hz) resolution magnetic field data from Geotail, we identified several large-amplitude FTEs, some of which are shown in Figure 4 along with simultaneous MMS-1 observations. Here *LMN* coordinates are determined for each spacecraft and each of the three intervals in Figure 4 by MVAB constraining that the average normal magnetic field component is zero $\langle B_N \rangle = 0$ [*Sonnerup and Scheible*, 1998]. All these FTEs, generated during quasi-continuous extended reconnection, had negative to positive B_N variations and were embedded in southward jets (Figures 4b and 4g), indicating that they were traveling

Table 1. Axial Orientation of the FTE Flux Rope or Tube From Multiple Triangulation Analysis (MTA)

Event ID[a]	GSM Components of the Axis
FTE1 (~0831:20 UT)	(0.4734, 0.8808, −0.0058)
FTE4 (~1025:30 UT)	(−0.5305, 0.8457, −0.0585)
FTE5 (~1033:40 UT)	(0.2166, 0.9566, −0.1974)

[a]See Figure 4 for event ID.

southward. They have peak-to-peak B_N durations of less than 1 min and thus belong to a category of relatively small FTEs [*Kawano and Russell*, 1996]. Hereafter, we call them as mesoscale FTEs, because both Geotail and MMS also observed a number of smaller-amplitude and shorter-duration bipolar B_N fluctuations that might be a manifestation of small-scale FTEs. They all have a maximum in the total pressure at the event center, as expected in the FTE bulge or magnetic flux rope where the force from the total pressure gradient balances magnetic tension of curved reconnected field lines [e.g., *Ieda et al*., 1998].

We point out that at least one of the mesoscale FTEs resulted from multiple X line reconnection. All FTEs seen by Geotail have a negative (duskward) B_M peak at their center, consistent with compression of the guide field in the surrounding region or Hall magnetic field in the outflow region southward of the site of asymmetric magnetopause reconnection [e.g., *Nakamura and Scholer*, 2000]. However, FTE1 in Figure 4 is preceded by a northward ion flow and positive B_M (dawnward field) component, both of which are signatures expected on the northern side of the reconnection site. It indicates that there was another X line on the southern side of the southward moving FTE1, consistent with FTE generation by multiple X line reconnection [e.g., *Hasegawa et al*., 2010]. This finding is significant in the sense that mesoscale flux ropes can form even during quasi-continuous reconnection, possibly in the vicinity of an active reconnection site as shown by *Hesse et al*. [1999] and *Eastwood et al*. [2007].

It is remarkable that MMS subsequently encountered no or only small-amplitude FTEs corresponding to those seen by Geotail. Since MMS was about 3 R_E ($\geq$350 ion inertial lengths in the magnetosheath) southward of Geotail (Figure 1) and the jet speed was 200–500 km/s (Figures 3 and 4b), it would take 1 ± 0.5 min for the FTEs to travel from the Geotail to MMS locations. Indeed, for FTE1, FTE2, FTE4, and FTE5 in Figure 4, MMS saw the corresponding bipolar B_N signatures in this range of time delay. However, the amplitudes of the bipolar B_N variations and of the field intensity and total pressure enhancements at MMS are all lower than seen by Geotail, except for FTE5. MMS was near the center of the magnetopause current sheet with small $|B_L|$ when the FTEs were expected to reach the MMS location (Figure 4e). We thus conclude that the smaller amplitudes are not due to MMS grazing the FTEs at locations far from the magnetopause center. For FTE5, the amplitude at MMS comparable to that at Geotail is likely due to MMS being closer to the current sheet center (smaller $|B_L|$).

One may think that the MMS observations of no or smaller-amplitude FTEs may be due to significant three-dimensional (3-D) elbow-shaped FTE structures, as expected for the Russell-Elphic model, that is, MMS was away from, or near the edge of, longitudinal sectors where FTEs were embedded in the magnetopause. However, we argue that the above features are in fact due to decay of the mesoscale FTEs. Here we use the multiple triangulation analysis (MTA) [*Zhou et al*., 2006] to estimate the axial orientations of FTE1, FTE4, and FTE5 identified distinctly by MMS. This method is essentially based on the four-spacecraft timing method [e.g., *Russell et al*., 1983] and assumes locally 2-D structures of the FTE flux tubes or ropes. The application to four-spacecraft measurements of magnetic field variations during these FTEs indicates that the FTE axes were oriented approximately in the longitudinal direction, i.e., roughly parallel to the equatorial X line (Table 1); the results are consistent with 2-D models of FTEs (see *Scholer* [1995] and *Paschmann et al*. [2013] for reviews of FTE models). We also point out that if FTEs had a constant cross-sectional size (amplitude) all over the magnetopause and were 3-D, i.e., had a short segment on the magnetopause, MMS and Geotail would have encountered large-amplitude FTEs with an equal detection probability. However, MMS detected a smaller number of large-amplitude FTEs: only one FTE seen by MMS (at ~1050:30 UT) had a field intensity peak exceeding 55 nT, while Geotail saw a total of nine such FTEs (FTEs 1–4 in Figure 4, and those at 0732:20 UT, 0827:00 UT, 1048:10 UT, 1106:00 UT, and 1150:40 UT) during the 5 h interval in Figure 2. All these features suggest that the mesoscale FTEs decayed as they traveled southward along the magnetopause from the Geotail to MMS locations.

5. Summary and Discussion

The simultaneous observations by the Geotail and MMS spacecraft have shown that magnetopause reconnection can be active for hours and, at the same time, be extended over a distance more than 10 R_E under

southward IMF conditions. The reconnection jets expanded into the magnetosphere with distance from the equatorial X line. Mesoscale flux transfer events (FTEs) with durations ≤1 min were encountered by Geotail near the equatorial plane, but no or only weaker amplitude corresponding FTEs were identified by MMS at midlatitudes ≥350 ion inertial lengths southward of Geotail. The observations are consistent with spatial decay of mesoscale FTEs as they are entrained in the southward jets of quasi-continuous spatially extended magnetopause reconnection. To the best of our knowledge, this is the first time that in situ observations in a single event have revealed the properties of magnetopause reconnection in all four-dimensional space time: prolonged reconnection, jet broadening along the normal, longitudinally extended X line, and latitudinal FTE evolution.

Although mesoscale FTEs generated during quasi-continuous reconnection appear to decay over the course of poleward transport, it is known that large-scale FTEs with cross-sectional diameters of order 1 R_E are often observed at high latitudes during continuous as well as noncontinuous reconnection intervals [e.g., *Phan et al*., 2004; *Wang et al*., 2005]. Transient magnetic signatures, likely corresponding to low-latitude FTEs, have been seen by the Cluster spacecraft in the lobe poleward of the cusp [*Thompson et al*., 2004]. Global MHD and kinetic simulations also show that FTEs tend to grow larger as they travel along the magnetopause [*Omidi and Sibeck*, 2007; *Dorelli and Bhattacharjee*, 2009]. Therefore, the spatial decay of FTEs may occur only for those of mesoscale or during quasi-continuous, rather than intermittent, reconnection. Such decay could be a manifestation of disentanglement or relaxation of tangled or colliding reconnected flux tubes constituting the FTEs [*Tan et al*., 2011], possibly through secondary reconnection in the outflow as seen in kinetic simulations [*Lapenta et al*., 2015]. These processes may be needed for the system to reach a lower energy state and for the dayside reconnected field lines to be transported toward the magnetotail.

We found no intervals on this day when a large-amplitude mesoscale FTE was observed by MMS in the burst mode. However, high time resolution measurements with MMS would make it possible to reveal complex topological structures of FTE field lines, as reported by *Pu et al*. [2013] and *Zhong et al*. [2013], and to study microphysical processes that may play a role in the FTE evolution and transport. Such processes include reconnection at the center of FTE flux ropes, which *Øieroset et al*. [2014] have attempted to analyze, and breakup of mesoscale FTEs into even smaller FTEs or flux ropes. Further studies are needed to fully understand how FTEs regulate transfer of solar wind plasmas and energy into the magnetosphere.

Acknowledgments
The Geotail data are available from DARTS: https://darts.isas.jaxa.jp/stp/geotail/, Wind data are from CDAWeb, and MMS data are available from the MMS Science Data Center: https://lasp.colorado.edu/mms/sdc/. We used the FPI data v2.1.0 and FGM data v4.18.0. IRAP contribution to MMS was supported by CNES. The work by H.H. was supported by JSPS Grant-in-Aid for Scientific Research KAKENHI 15K05306.

References

Burch, J. L., T. E. Moore, R. B. Torbert, and B. L. Giles (2016), Magnetospheric Multiscale overview and science objectives, *Space Sci. Rev.*, *199*, 5–21, doi:10.1007/s11214-015-0164-9.

Dorelli, J. C., and A. Bhattacharjee (2009), On the generation and topology of flux transfer events, *J. Geophys. Res.*, *114*, A06213, doi:10.1029/2008JA013410.

Dungey, J. W. (1961), Interplanetary magnetic field and the auroral zones, *Phys. Rev. Lett.*, *6*, 47–48.

Dunlop, M. W., et al. (2011), Extended magnetic reconnection across the dayside magnetopause, *Phys. Rev. Lett.*, *107*, 025004, doi:10.1103/PhysRevLett.107.025004.

Eastwood, J. P., T.-D. Phan, F. S. Mozer, M. A. Shay, M. Fujimoto, A. Retinò, M. Hesse, A. Balogh, E. A. Lucek, and I. Dandouras (2007), Multi-point observations of the Hall electromagnetic field and secondary island formation during magnetic reconnection, *J. Geophys. Res.*, *112*, A06235, doi:10.1029/2006JA012158.

Frey, H. U., T. D. Phan, S. A. Fuselier, and S. B. Mende (2003), Continuous magnetic reconnection at Earth's magnetopause, *Nature*, *426*, 533–537.

Fuselier, S. A. (1995) Kinetic aspects of reconnection at the magnetopause, in *Physics of the Magnetopause*, edited by P. Song, B. U. Ö. Sonnerup, and M. F. Thomsen, pp. 181–187, AGU, Washington, D. C., doi 10.1029/GM090p0181.

Hasegawa, H., A. Retinò, A. Vaivads, Y. Khotyaintsev, R. Nakamura, T. Takada, Y. Miyashita, H. Rème, and E. A. Lucek (2008), Retreat and reformation of X-line during quasi-continuous tailward-of-the-cusp reconnection under northward IMF, *Geophys. Res. Lett.*, *35*, L15104, doi:10.1029/2008GL034767.

Hasegawa, H., et al. (2010), Evidence for a flux transfer event generated by multiple X-line reconnection at the magnetopause, *Geophys. Res. Lett.*, *37*, L16101, doi:10.1029/2010GL044219.

Hesse, M., K. Schindler, J. Birn, and M. Kuznetsova (1999), The diffusion region in collisionless magnetic reconnection, *Phys. Plasmas*, *6*, 1781–1795.

Ieda, A., S. Machida, T. Mukai, Y. Saito, T. Yamamoto, A. Nishida, T. Terasawa, and S. Kokubun (1998), Statistical analysis of the plasmoid evolution with Geotail observations, *J. Geophys. Res.*, *103*(A3), 4453–4465, doi:10.1029/97JA03240.

Kawano, H., and C. T. Russell (1996), Survey of flux transfer events observed with the ISEE 1 spacecraft: Rotational polarity and the source region, *J. Geophys. Res.*, *101*, 27,299–27,308, doi:10.1029/96JA02703.

Lapenta, G., S. Markidis, M. V. Goldman, and D. L. Newman (2015), Secondary reconnection sites in reconnection-generated flux ropes and reconnection fronts, *Nat. Phys.*, *11*, 690–695, doi:10.1038/nphys3406.

Lavraud, B., et al. (2013), Asymmetry of magnetosheath flows and magnetopause shape during low Alfvén Mach number solar wind, *J. Geophys. Res. Space Physics*, *118*, 1089–1100, doi:10.1002/jgra.50145.

Mukai, T., S. Machida, Y. Saito, M. Hirahara, T. Terasawa, N. Kaya, T. Obara, M. Ejiri, and A. Nishida (1994), The low energy particle (LEP) experiment on board the Geotail satellite, *J. Geomagn. Geoelectr.*, *46*, 669–692, doi:10.5636/jgg.46.669.

Nakamura, M. S., and M. Scholer (2000), Structure of the magnetopause reconnection layer and of flux transfer events: Ion kinetic effects, *J. Geophys. Res.*, *105*, 23,179–23,191, doi:10.1029/2000JA900101.
Øieroset, M., D. Sundkvist, C. C. Chaston, T. D. Phan, F. S. Mozer, J. P. McFadden, V. Angelopoulos, L. Andersson, and J. P. Eastwood (2014), Observations of plasma waves in the colliding jet region of a magnetic flux rope flanked by two active X lines at the subsolar magnetopause, *J. Geophys. Res. Space Physics*, *119*, 6256–6272, doi:10.1002/2014JA020124.
Omidi, N., and D. G. Sibeck (2007), Flux transfer events in the cusp, *Geophys. Res. Lett.*, *34*, L04106, doi:10.1029/2006GL028698.
Paschmann, G., M. Øieroset, and T. Phan (2013), In-situ observations of reconnection in space, *Space Sci. Rev.*, *47*, 309–341, doi:10.1007/978-1-4899-7413-6_12.
Phan, T. D., et al. (2004), Cluster observations of continuous reconnection at the magnetopause under steady interplanetary magnetic field conditions, *Ann. Geophys.*, *22*, 2355–2367.
Phan, T. D., H. Hasegawa, M. Fujimoto, M. Øieroset, T. Mukai, R. P. Lin, and W. R. Paterson (2006), Simultaneous Geotail and Wind observations of reconnection at the subsolar and tail flank magnetopause, *Geophys. Res. Lett.*, *33*, L09104, doi:10.1029/2006GL025756.
Pollock, C., et al. (2016), Fast plasma investigation for Magnetospheric Multiscale, *Space Sci. Rev.*, *199*, 331–406, doi:10.1007/s11214-016-0245-4.
Pu, Z. Y., J. Raeder, J. Zhong, Y. V. Bogdanova, M. Dunlop, C. J. Xiao, X. G. Wang, and A. Fazakerley (2013), Magnetic topologies of an in vivo FTE observed by Double Star/TC-1 at Earth's magnetopause, *Geophys. Res. Lett.*, *40*, 3502–3506, doi:10.1002/grl.50714.
Russell, C. T., and R. C. Elphic (1978), Initial ISEE magnetometer results: Magnetopause observations, *Space Sci. Rev.*, *22*, 681–715.
Russell, C. T., M. M. Mellott, E. J. Smith, and J. H. King (1983), Multiple spacecraft observations of interplanetary shocks: Four spacecraft determination of shock normals, *J. Geophys. Res.*, *88*, 4739–4748, doi:10.1029/JA088iA06p04739.
Russell, C. T., et al. (2016), The Magnetospheric Multiscale magnetometers, *Space Sci. Rev.*, *199*, 189–256, doi:10.1007/s11214-014-0057-3.
Scholer, M. (1995), Models of flux transfer events, in *Physics of the Magnetopause*, edited by P. Song, B. U. O. Sonnerup, and M. F. Thomsen, pp. 235–245, AGU, Washington, D. C., doi:10.1029/GM090p0235.
Shue, J.-H., et al. (1998), Magnetopause location under extreme solar wind conditions, *J. Geophys. Res.*, *103*(A8), 17,691–17,700, doi:10.1029/98JA01103.
Sibeck, D. G., and G. L. Siscoe (1984), Downstream properties of magnetic flux transfer events, *J. Geophys. Res.*, *89*, 10,709–10,715, doi:10.1029/JA089iA12p10709.
Sonnerup, B. U. Ö., and M. Scheible (1998), Minimum and maximum variance analysis, in *Analysis Methods for Multi-Spacecraft Data*, edited by G. Paschmann and P. W. Daly, chap. 8, pp. 185–220, ESA Publ., Noordwijk, Netherlands.
Sonnerup, B. U. Ö., I. Papamastorakis, G. Paschmann, and H. Lühr (1987), Magnetopause properties from AMPTE/IRM observations of the convection electric field: Method development, *J. Geophys. Res.*, *92*, 12,137–12,159, doi:10.1029/JA092iA11p12137.
Tan, B., Y. Lin, J. D. Perez, and X. Y. Wang (2011), Global-scale hybrid simulation of dayside magnetic reconnection under southward IMF: Structure and evolution of reconnection, *J. Geophys. Res.*, *116*, A02206, doi:10.1029/2010JA015580.
Thompson, S. M., M. G. Kivelson, K. K. Khurana, A. Balogh, H. Rème, A. N. Fazakerley, and L. M. Kistler (2004), Cluster observations of quasi-periodic impulsive signatures in the dayside northern lobe: High-latitude flux transfer events?, *J. Geophys. Res.*, *109*, A02213, doi:10.1029/2003JA010138.
Wang, J., M. W. Dunlop, Z. Y. Pu, X. Z. Zhou, X. G. Zhang, Y. Wei, and S. Y. Fu (2007), TC1 and Cluster observation of an FTE on 4 January 2005: A close conjunction, *Geophys. Res. Lett.*, *34*, L03106, doi:10.1029/2006GL028241.
Wang, Y. L., et al. (2005), Initial results of high-latitude magnetopause and low-latitude flank flux transfer events from 3 years of Cluster observations, *J. Geophys. Res.*, *110*, A11221, doi:10.1029/2005JA011150.
Zhong, J., et al. (2013), Three-dimensional magnetic flux rope structure formed by multiple sequential X-line reconnection at the magnetopause, *J. Geophys. Res. Space Physics*, *118*, 1904–1911, doi:10.1002/jgra.50281.
Zhou, X.-Z., Q.-G. Zong, Z. Y. Pu, T. A. Fritz, M. W. Dunlop, Q. Q. Shi, J. Wang, and Y. Wei (2006), Multiple triangulation analysis: Another approach to determine the orientation of magnetic flux ropes, *Ann. Geophys.*, *24*, 1759–1765.

Erratum

In the originally published version of this article, in Section 1, FPI was incorrectly defined as "Fabry-Perot interferometer". The definition has since been corrected to "Fast Plasma Investigation". This version may be considered the authoritative version of record.